Scanning Microscopy

Volume 5 | Number 3 Article 28

8-26-1991

# Elemental Analysis and Fine Structure of Mitochondrial Granules in Growth Plate Chondrocytes Studied by Electron Energy Loss Spectroscopy and Energy Dispersive X-Ray Microanalysis

Joanna Wroblewski
*Karolinska Institutet*

Romuald Wróblewski
*Karolinska Institutet*

Claudie Mory
*Université Paris-Sud*

Christian Colliex
*Université Paris-Sud*

Follow this and additional works at: https://digitalcommons.usu.edu/microscopy

Part of the Biology Commons

## Recommended Citation

Wroblewski, Joanna; Wróblewski, Romuald; Mory, Claudie; and Colliex, Christian (1991) "Elemental Analysis and Fine Structure of Mitochondrial Granules in Growth Plate Chondrocytes Studied by Electron Energy Loss Spectroscopy and Energy Dispersive X-Ray Microanalysis," *Scanning Microscopy*: Vol. 5 : No. 3 , Article 28.
Available at: https://digitalcommons.usu.edu/microscopy/vol5/iss3/28

This Article is brought to you for free and open access by the Western Dairy Center at DigitalCommons@USU. It has been accepted for inclusion in Scanning Microscopy by an authorized administrator of DigitalCommons@USU. For more information, please contact digitalcommons@usu.edu.

Scanning Microscopy, Vol. 5, No. 3, 1991 (Pages 885-894)
Scanning Microscopy International, Chicago (AMF O'Hare), IL 60666 USA

0891-7035/91$3.00+.00

# ELEMENTAL ANALYSIS AND FINE STRUCTURE OF MITOCHONDRIAL GRANULES IN GROWTH PLATE CHONDROCYTES STUDIED BY ELECTRON ENERGY LOSS SPECTROSCOPY AND ENERGY DISPERSIVE X-RAY MICROANALYSIS

**Joanna Wroblewski[1]*, Romuald Wróblewski[2], Claudie Mory[3] and Christian Colliex[3]**

[1] Department of Medical Cell Genetics and [2]Department of Pathology, Karolinska Institutet, S-104 01 Stockholm, Sweden.
[3]Laboratoire de Physique des Solides, Bldg. 510, Université Paris-Sud,F-91405 Orsay, France.

(Received for publication November 21, 1990, and in revised form August 26, 1991)

## Abstract

Electron energy loss spectrometry - EELS, and energy dispersive X-ray microanalysis - XRMA, were used to study the elemental composition of mitochondrial dense granules - mdg. The study was performed on dry cut thin sections (80-200 nm) of freeze-dried and low temperature embedded cartilage. Results obtained by means of XRMA clearly showed high phosphorus and calcium content in the mdg. Using EELS at 100 kV primary voltage we found that small concentrations of elements (i.e. below typically 1 % atomic weight) are difficult to analyze and map, this especially in sections thicker than 50-60 nm. Surprisingly, analysis of calcium can be successfully performed on thicker sections though the edge lies above the carbon K edge while this is not possible for the phosphorus edge which is located at lower energies. This is likely due to the edge shapes (sharp for calcium and delayed for phosphorus), and to the more intense contribution of multiple low loss scattering in the background for phosphorus between 100 and 130 eV. By means of EELS elemental mapping a centrally located core was found in numerous mdg. In the calcium map the signal was strongest in the middle of mdg which corresponds to the area of reduced carbon signal. We found that carbon maps might be used for high resolution structural studies of chemically unfixed and anhydrously processed biological tissues. As carbon is the main constituent of Lowicryl resin its distribution is reversed to the distribution of biological tissue in which the proportion of carbon is lower, but is proportional to water content in the specimen *in vivo*. Use of EELS in combination with electron microscope with accelerating voltages in range of 140-200 kV together with anhydrous techniques of the tissue preparation will provide a new type of information which might lead to better understanding of the etiology and function of small structures in the cell.

Key words: electron energy loss spectroscopy, X-ray microanalysis, cartilage, mitochondrial granules, Lowicryl resin, elemental mapping

* Address for correspondence:
Joanna Wroblewski
Department of Medical Cell Genetics, Medical Nobel Institute, Karolinska Institutet, S-104 01 Stockholm, Sweden
Phone No.: +46 (8) 728 73 26
Fax No.: +46 (8) 34 58 20

## Introduction

Mitochondria containing dense granules have been reported in a variety of tissues, among others in tissues involved in the calcification and pathological processes. Mitochondrial dense granules (mdg) can be found in tissues conventionally processed for electron microscopy as well as in cryofixed material without previous chemical fixation or contrasting. Mdg are often regarded as an artefact in conventional preparations, that occurs due to the cell metabolism changes prior to fixation. Their number can be increased by calcium loading prior to fixation (Blaineau and Nicaise 1976) or by adding calcium to the fixative (Sampson et al. 1970). Calcium loading prior to fixation may also cause disappearance of normally occurring mdg (Peachey 1964). In cryosections mdg are in many cases regarded as an artefact caused by post-mortem changes or freeze-drying of the cryosections. The analysis of such mdg have revealed high phosphorus and calcium content. The same elemental composition of mdg has been detected in numerous normal and pathological tissues, where occurrence of mdg represents most probably the actual *in vivo* situation. Microanalysis of dense granules has shown that phosphorus or calcium may be found alone or together in different tissues processed using different preparation methods. Phospholipids are likely to be the main component of such granules (Barnard and Ruusa 1979). Mdg are also present in tissues which have been cryofixed and cryosubstituted without osmium in the substitution media (Nicaise et al. 1989).

The present study has been undertaken to investigate elemental composition and ultrastructure of mdg in rat rib growth plate chondrocytes prepared by low temperature vacuum embedding technique. Electron energy loss spectroscopy and energy dispersive X-ray microanalysis have been used for elemental analysis and mapping.

## Materials and Methods

### Freezing

Rat rib growth plates were dissected from deeply anesthetized 4-week-old rats of Sprague-Dawley strain. Immediately after dissection, blocks of tissue, about 1 $mm^3$ large, were cryofixed by plunging them directly into liquid propane (-189 °C) or ethane (-171 °C) cooled by liquid nitrogen ($LN_2$). The frozen samples were routinely stored in $LN_2$ prior to further processing.

### Dehydration and embedding

Samples of frozen tissue, placed in plastic vials filled

with $LN_2$ (Nunc cryotubes) were transferred to the precooled chamber of the modified Low Temperature Vacuum Embedding Processor (LTVEP) (Wroblewski and Wroblewski 1984). The processor was put under vacuum when the specimen temperature reached -160 °C and the liquid nitrogen was evaporated completely from the vials to avoid the formation of melting nitrogen. The temperature of the freeze-drying chamber was then slowly raised to about -95 °C for 10-12 hours. During the subsequent 24 hours, the temperature was raised gradually to -80 °C. The vacuum in the freeze-drier was kept below $10^{-5}$ Torr. The final vacuum was in the range of $10^{-6}$ Torr. The condenser temperature was kept at -120 °C for the first 16 hours of freeze-drying. After freeze-drying was completed, Lowicryl embedding medium was introduced to the vials containing the specimens without breaking the vacuum or altering the temperature in the cryochamber (Wroblewski and Wroblewski 1984). The tissues were impregnated with resin overnight. Lowicryl HM23 was polymerized at -80 °C by illumination with UV light of 360 nm, without breaking the vacuum or changing the temperature conditions of the freeze-drying apparatus.

### Sectioning

Thin sections (of nominal thickness 80-200 nm) of freeze-dried embedded material were cut at ambient or at low temperature with a glass knife on a Reichert cryoultramicrotome. To prevent redistribution and loss of ions, the sections were collected dry from the knife edge using an eyelash. They were then transferred to naked or formvar-film coated EM-grids and pressed to the grids with a polished silver rod. Naked grids were made "sticky" by dipping them in gummi arabicum solution. Some sections were cut on glycerol or water surface to evaluate elemental and morphological changes caused by these trough liquids. When glycerol was used it was poured from a new bottle directly before cutting in order to prevent hydration. The sections were collected from the glycerol or water surface immediately after cutting. Glycerol was removed from the sections with filter paper or pure ethanol. The grids were stored dry, over molecular sieves, before analysis.

In a control experiment conventionally cut ultrathin (50 nm) sections of resin embedded eye lens containing crystalline inclusions, which are not water soluble, were used in purpose of establishing the detection efficiency for phosphorus and calcium.

### Electron microscopy and X-ray microanalysis

Thin sections were analyzed in a JEOL 1200CX electron microscope with a scanning attachment. Energy dispersive X-ray microanalysis was carried out with a Tracor 5500 - analytical system. Lowicryl sections were observed and analyzed at 100 or 120 kV. The cold finger and cold trap were used during observation and analysis.

### Electron Energy Loss Spectroscopy and Imaging

Electron energy loss spectroscopy (EELS) and imaging were performed using a dedicated VG-HB501 scanning transmission electron microscope coupled with a Gatan EELS spectrometer and a Kevex energy dispersive analyser. Observations were made at 100 kV accelerating voltage.

## Results

### X-ray microanalysis

Dry cut sections of epiphyseal plates were analyzed unstained in the scanning transmission mode (STEM) of the conventional microscope. In some of the proliferating chondrocytes the mitochondria were electron dense and the mdg appeared as opaque clusters of granules (see Fig. 1a-b). The mitochondrial membranes were difficult to delineate in LTVEP prepared samples. The gross morphology of mdg in freeze-dried and embedded preparations was in general worse than that found in the conventionally chemically fixed and embedded material. X-ray microanalysis of the mdg revealed high concentrations of phosphorus and calcium (Fig. 2a). Also small amounts of sodium, magnesium, sulphur, chlorine and potassium were detected within the mdg. In mitochondrial matrix, surrounding the mdg, these elements were also present, however, at much lower concentrations. Analyses were also performed on nuclei, cytoplasm and areas occupied only by pure Lowicryl resin (next to the cartilage). In the elemental spectra from the nuclei a prominent phosphorus and a potassium peak were present (data not shown). No elements detectable by X-ray microanalysis were present in the resin outside the tissue.

In the present investigation the cutting problems (compression) encountered sometimes at ambient temperature, could be reduced by lowering the sectioning temperature. For collection of sections cut at room temperature, the "sticky" naked grids were more convenient, and gave better stability of the sections under the electron beam.

In order to evaluate redistribution and loss of ions and to obtain thinner sections, some blocks were cut on glycerol or water surface. In such sections a significant loss and redistribution of elements were detected. The most prominent was the loss of calcium from the mdg. Losses of calcium were accompanied by phosphorus, chlorine and potassium losses (Fig. 2b-c). The phosphorus to calcium ratio in mdg in dry cut sections was 1:1 and in sections cut onto glycerol 1:0.2. In sections cut on water and immediately picked up the losses of calcium, chlorine and potassium from the mdg were almost complete (Fig. 2c).

### Electron energy loss spectroscopy

To improve the spatial resolution and sensitivity of analysis of calcium (normally occurring at low concentration in cytoplasm and mitochondria) dry cut sections were analysed in the VG-HB501 scanning transmission electron microscope. The annular dark field image was similar to the conventional image, however, the stability of the sections was much better, probably due to the reduced local heating under the very small probe delivered by the field emission gun in the dedicated STEM.

Electron energy loss spectra from the dense granules show a distinct calcium $L_{23}$ peak at 347-350 eV superimposed on the carbon K edge (Fig. 3). However, phosphorus (easily identified using XRMA) is difficult to detect. The phosphorus $L_{23}$ signal at 135-136 eV is actually hidden in the background due to multiple scattering caused by the section thickness and it is therefore difficult to reveal it with the standard background subtraction program using a two parameter power law model such as described by Egerton (1986). The section thickness (estimated by us during cutting to be in the range of 70-90 nm) is in fact substantially greater when estimated from the low loss region in the EELS spectrum: it generally amounts to 1.5 to 2 inelastic mean free paths, which corresponds to about 150 to 200 nm. This gives rise to important changes in the background shape over the energy loss range used for modelling before the phosphorus threshold, so that the simple model is no longer valid. Moreover, the section thickness causes multiple scattering on top of the carbon K edge, which makes the estimation of all superimposed edges such as the calcium $L_{23}$ and the nitrogen K ones as illustrated in Fig. 3a more difficult. These effects diminish the possibility of

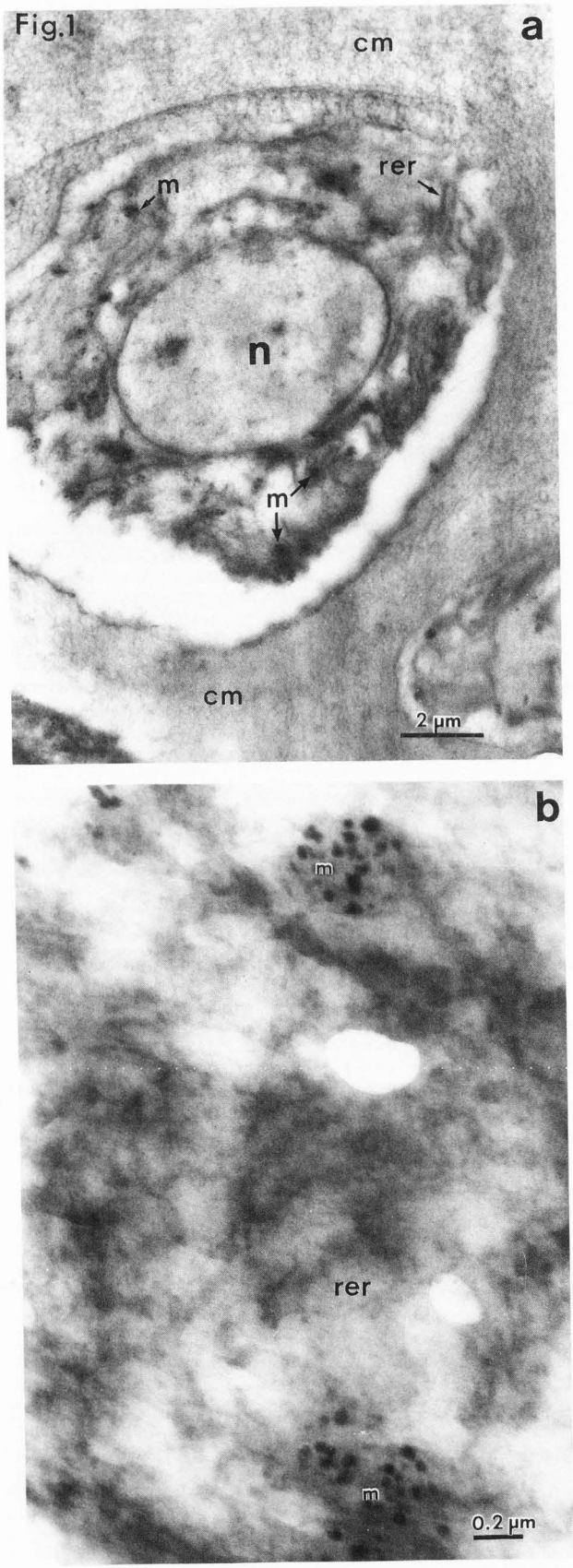


**Fig. 1 a-b:** Transmission electron micrograph of cells in the epiphyseal plate in rat rib growth plate. **a.** Low magnification electron micrograph of unstained section of low temperature embedded cartilage cut on dry knife edge. The cartilage matrix-cm, rough endoplasmic reticulum-rer, mitochondria-m, and nucleus-n can be easily identified. **b.** Higher magnification of the same section as in **a** displaying mitochondria with dense granules (arrows).

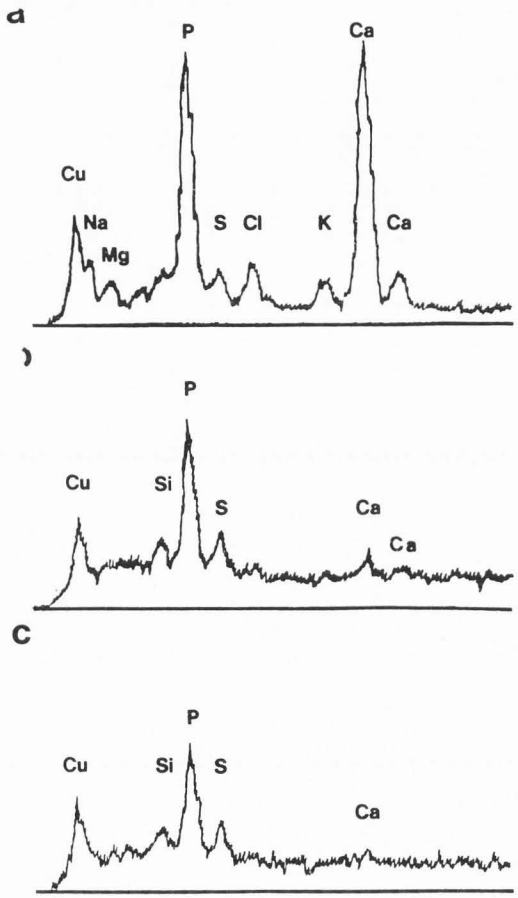


**Fig. 2 a-c:** X-ray spectra demonstrating effect of cutting of sections on final elemental concentration of mitochondrial dense granule. **a.** Sections cut on dry knife edge. **b.** Sections cut on glycerol. **c.** Sections cut on water surface. Vertical scale 1 000.

identifying or imaging elements of interest, such as nitrogen and phosphorus.

Elemental maps of carbon and calcium have been recorded. The method used consists of extrapolating for each pixel individually, the background contribution estimated from two or three filtered images recorded with energy losses below the edge of interest (Jeanguillaume et al. 1978, Bonnet et al. 1988), see Fig. 4. A simultaneously recorded annular dark field image of mdg is also included. It is more sensitive to mass thickness features and displays with rather good spatial resolution the position and shape of each granule. Moreover there exists some hint of the presence of a dense core in the middle of a few mdg with a diameter of

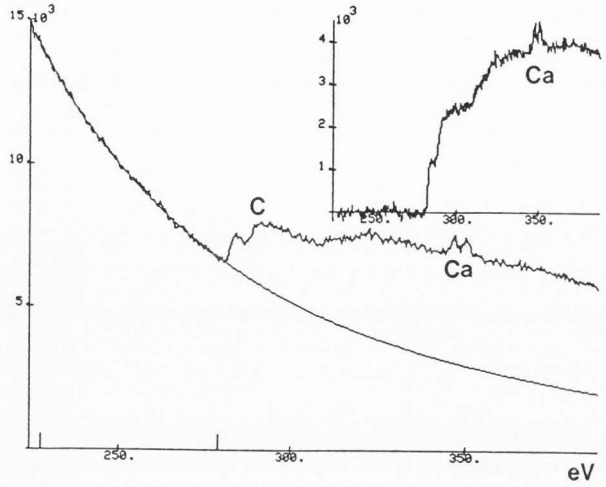


**Fig. 3:** EELS spectra from an assembly of mdg clearly showing the presence of the carbon and calcium edges.

approximately half of the whole mdg. When considering the elemental maps, the reverse contrast observed in the carbon image provides the same type of morphological information through a reduction of the carbon signal. In the calcium map the signal is strongest in the middle of the granule, which also corresponds to the area of reduced carbon signal. At that point it is uncertain whether this is associated with a real change in elemental composition, which would require an extra scaling procedure, with the unscattered signal for instance. It would, however, be in agreement with some observed changes of the phosphorus to calcium ratio in XRMA spectra from the inner and outer parts of mdgs. The calcium concentration is lower in the mitochondrial matrix and in the cytoplasm and thus impossible to image.

In order to evaluate quantitatively the detection limits for different EELS signals involved through this study, in a control experiment we analysed 50 nm thick sections (obtained by cutting on to water) of the crystalline inclusions in eye lens. The spectra (Fig. 5) clearly display all involved edges, i.e. along increasing energy losses, phosphorus $L_{23}$ at 135 eV, carbon K edge at 284 eV, calcium $L_{23}$ at 350 eV, and oxygen K at 532 eV. After conventional background stripping, fine structures are visible on all of them. Using the quantitation program developed by Trebbia (1988), one evaluates the relative atomic concentration of these elements as carbon (69 %), phosphorus (5 %), calcium (6.5 %) and oxygen (20 %), in satisfactory agreement with hydroxyapatite ($Ca_3(PO_4)_2$) embedded within an organic matrix. Detection limits of the order of 0.5 % phosphorus and 0.3 % calcium can be evaluated for such a spectrum on an embedded inclusion. Moreover the present conditions have made it possible to perform elemental mapping for phosphorus, oxygen and calcium in the carbonaceous matrix. These results concern the thin sections obtained by sectioning on water which could be employed only because the crystalline inclusions are not water soluble.

## Discussion

### Biological significance

The intracellular distribution of calcium has been the subject of numerous investigations. The data obtained by biochemical or chemical methods on the different cell fractions after zonal centrifugation showed high calcium concentrations in the mitochondrial fraction. More recent data, however, revealed rather low calcium concentrations in the intact mitochondria (Barnard 1981, Somlyo 1985). However, in normal non affected tissues, high calcium levels in mitochondria and in mitochondrial dense granules can be found in few cell types. In numerous reports, the presence of the calcium rich mdg has been caused by cell damage either in pathological conditions (Somlyo et al. 1977) or due to tissue preparation artefacts (Sevéus et al. 1978). Blaineau and Nicaise 1976 have shown that the number of mdg increases in case of moderate loading with $Ca^{2+}$ prior to fixation. Barnard (1981) showed that mdg may contain phospholipids. Hertsens et al. (1986) demonstrated cytochrome C oxidase activity in mdg of rat heart mitochondria by using post-embedding immunocytochemistry.

The presence of mdg in chondrocytes of epiphyseal plates has often been associated with the mineralization process. Stufin et al. (1971) analyzed mdg from hypertrophic chondrocytes from costal growth plates and found P and Ca to be present in all analyzed mdg but not in the mitochondrial matrix. In this early investigation performed on conventionally processed material the authors could not decide if mdg are present *in vivo* or are a preparation artefact. Wróblewski et al. (1981, 1984) investigated morphology and elemental composition of smallest striated muscle in mammalian body, *m. stapedius*. In conventionally processed stapedius muscle, dense granules were present in all mitochondria. The mdg which appeared as very dense inclusions were dissolved from the sections after 2 min incubation with hydrogen peroxide. X-ray microanalysis performed within thick cryosections on areas densely packed with mitochondria revealed high P and Ca signals. The study was followed by analysis of mdg in thin cryosections (Wróblewski et al. 1984, Wróblewski 1989).

In cell injury the development of the mdg with calcium phosphate precipitates depends on the nature of original insult as suggested by Trump and Berezesky (1986). These authors regard the process of calcium accumulation as an active process, which requires mitochondrial function. Mdg with P and Ca accumulations do not occur if the injury inhibits active transport in mitochondria. Total ischemia, anoxia or poisoning with respiratory inhibitors (cyanide or carbonmonoxide) result in cell death and formation of dense granules which do not contain Ca or P. In lethal insults where the toxin primarily modifies the cell membrane or organelles other than mitochondria leaving the mitochondria more or less intact, the mitochondria show calcium phosphate containing dense granules when cell death occurs. Calcium precipitation in mitochondria commonly occurs in situations where reflow to an area of ischemia is permitted such as at the edges of infarcts, and in complete anoxia or ischemia followed by reflow or reoxygenation (Trump and Berezesky 1986). Analysis of calcium content by XRMA is problematic because in many compartments calcium content stays under the sensitivity limits. Also the presence of a high potassium concentration and low calcium renders quantitation difficult due to the overlap of the potassium $K_\beta$ and calcium $K_\alpha$ lines. However, Somlyo (1985) reported calcium levels down to few tenths of mmol per kg dry weight.

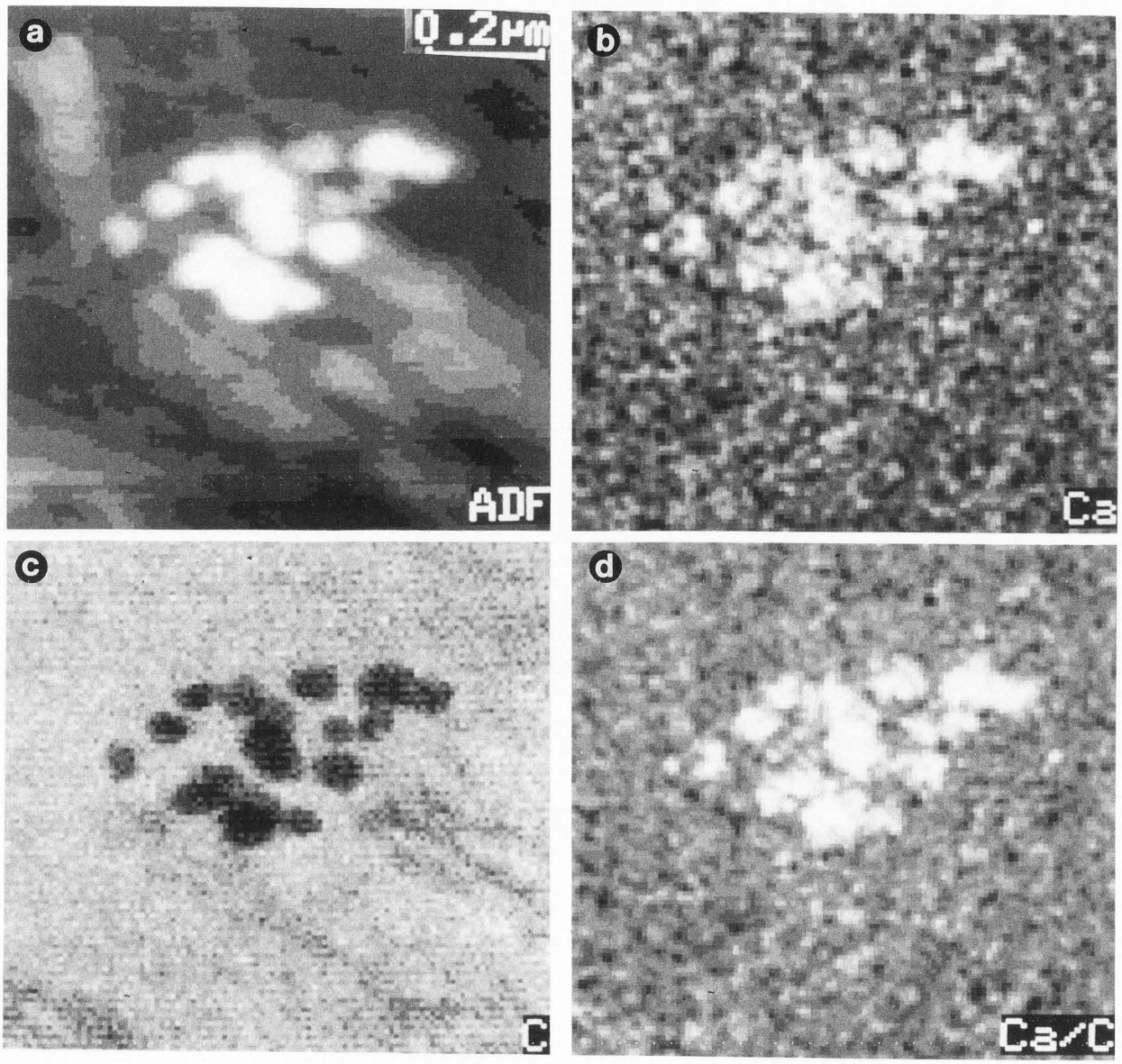


**Fig. 4a-d:** Micrographs of an assembly of mitochondrial dense granules: (**a**) annular dark field image; (**b**) calcium map; (**c**) carbon map; (**d**) calcium/carbon ratio map.

**Electron energy loss spectroscopy - limits in terms of sensitivity for different elements in relation to the section thickness**

The analysis of the crystalline inclusions in eye lens performed on 50 nm thick plastic sections compared to analysis of thicker dry-cut sections confirms that the major difficulty encountered in the elemental analysis and mapping of the mdg in the mitochondria is due to the too large thickness of a section carefully prepared for maintaining the chemical integrity of the specimen. It illustrates one of the main problems in tissue preparation for EELS. Thin sections of biological material are difficult to obtain by means of dry cutting. Cutting on a liquid surface produces thinner sections suitable for EELS, but with false information concerning elemental composition due to the losses and redistribution of element during contact with trough liquid (glycerol or water). Blaineau et al. (1987) compared the calcium content of molluscan glio-interstitial granules and found that if sections were collected on water 75 % of calcium was lost in comparison with sections cut on glycerol. No comparison was, however, done with sections cut dry. Blaineau (Blaineau et al. 1987) found that a significant part of calcium was lost if the sections were floated on water for 5 minutes but not if the sections were collected immediately after cutting. Marshall (1980) reported an increase in the calcium content of sections collected on glycerol when compared to dry cut, which again indicates redistribution of calcium. The most reasonable explanation to the losses and redistribution of elements while cutting on glycerol is that glycerol due to it

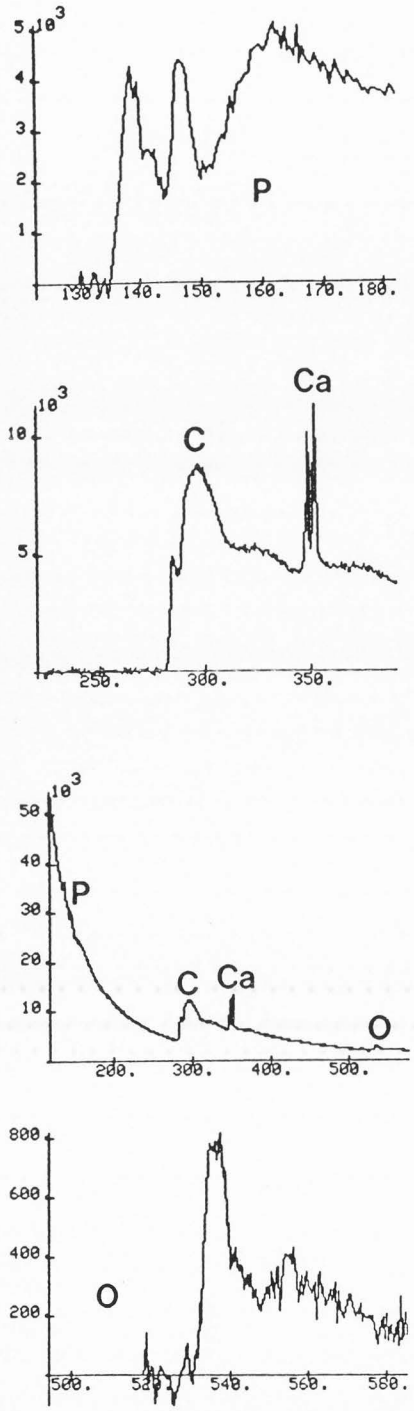


**Fig. 5:** Electron energy loss spectra from a reference crystalline inclusion in eye lens displaying the four dominant edges : phosphorus $L_{23}$, carbon K, calcium $L_{23}$, oxygen K, with some detailed fine structures in inserts, used for quantification and detectability in a control experiment.

hydrophily attracts water molecules from the environment resulting in a rather hydrous surface on which the sections float.

In the present state of the art, it may be simpler to solve the multiple scattering problem caused by the fact that dry cut sections are too thick, by using higher accelerating voltages (200-300 kV) rather than by improvements in the sectioning techniques.

One may also overcome this problem by developing more appropriate processing routines for sequences of filtered energy loss images recorded on thick specimens. To illustrate that point, Fig. 6 contains the full gallery of original filtered images recorded at higher magnification on an assembly of dense granules images. We show them for a double purpose: first they demonstrate the heterogeneity within individual granules. Secondly when varying the energy loss, they exhibit gradual changes in contrast which deserves further image processing. For instance, when crossing the phosphorus threshold, one notices a modification in the contrast from a hollow type image of the granules to a filled one. This change cannot be revealed through the two parameter background subtraction which constitutes in this case a too restrictive assumption. The spatial distribution of phosphorus cannot be visualized because of the very low signal to noise ratio in the original filtered image and of a misfit of the power low model in the background area (between 120 and 135 eV). Such faint variations require more appropriate processing. Trebbia and Mory (1990) have recently applied factorial analysis of correspondence to this series of images. Most of the variance, measured along the principal axis, discriminates the images above the P edge (i.e. 150 and 163 eV) from the images below. When projected along this axis, the micrographs display white areas near the centre of the granules. This approach confirms, without specific reference to a mathematical model, the existence of a clear variation in signal between the pre- and post edge micrographs in the core of the dense granules. Though the processed image bears noticeable resemblance with a phosphorus element map, it is not yet fully established whether this is a map of phosphorus, or not.

Finally we want to emphasize the use of carbon maps for high resolution structural studies of chemically unfixed and anhydrously processed biological tissues. As carbon is the main constituent of Lowicryl resin its distribution is reversed to the distribution of biological tissue in which proportion of carbon is lower, but is proportional to water content in the specimen *in vivo*.

**Fig. 6**: Gallery of unprocessed energy filtered images on mdg required for the calculation of the phosphorus, carbon and calcium maps. Notice the small change in contrast when crossing the P $L_{23}$ edge at about 135 eV, the complete contrast reversal when crossing the carbon K edge at 284 eV. Finally the Ca $L_{23}$ signal appears as a weak change in contrast between 330 and 360 eV. In this energy loss domain, the mdg contrast is of negative type because most of the intensity is due to carbon. This negative contrast is due to the fact that an important fraction of the scattered electrons is transferred to the annular dark field detector when the beam is on the mdg and therefore lost for energy loss analysis by the spectrometer.

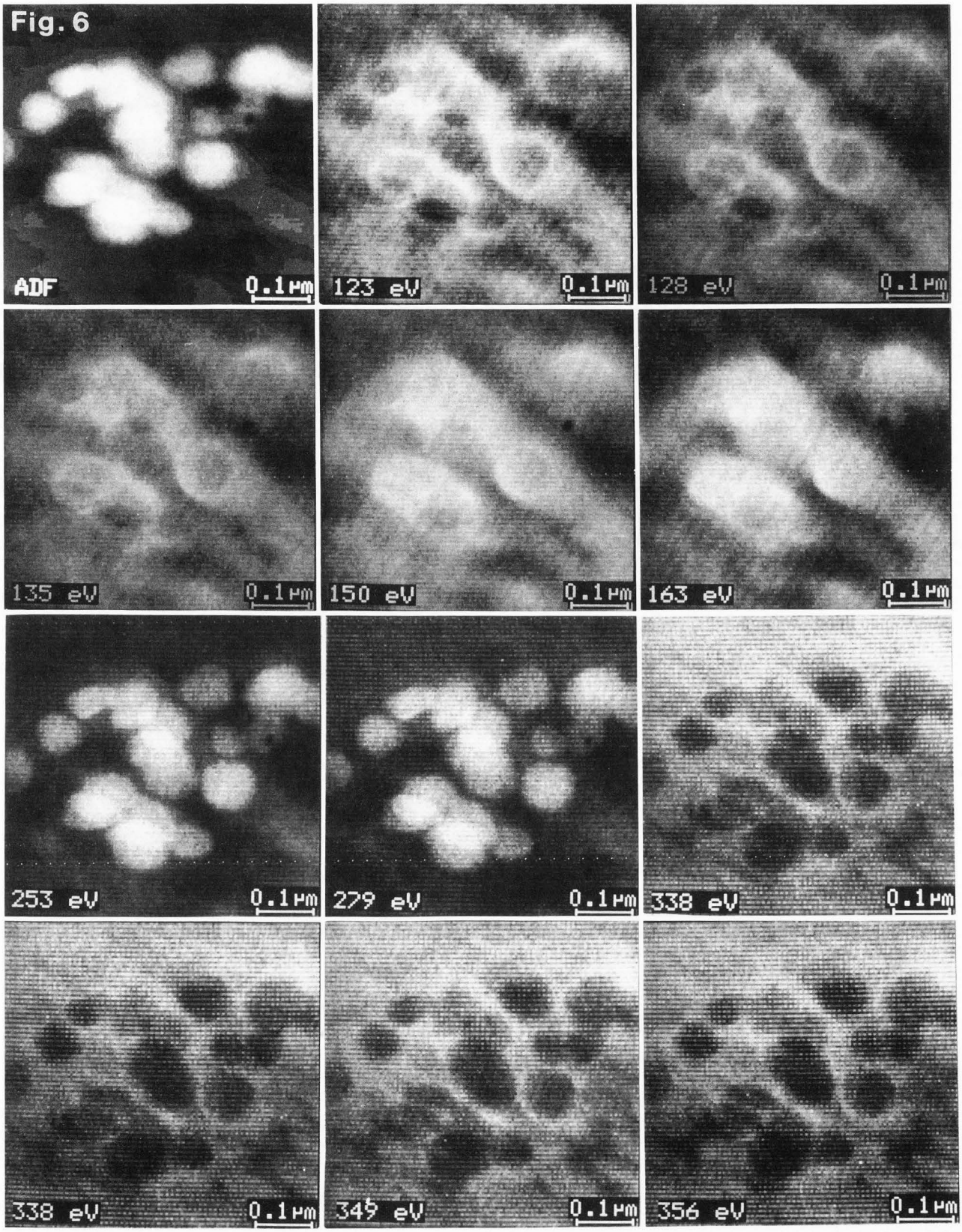
Fig. 6
ADF
0.1 μm
123 eV
0.1 μm
128 eV
0.1 μm
135 eV
0.1 μm
150 eV
0.1 μm
163 eV
0.1 μm
253 eV
0.1 μm
279 eV
0.1 μm
338 eV
0.1 μm
338 eV
0.1 μm
349 eV
0.1 μm
356 eV
0.1 μm

## Conclusions

It has been demonstrated that additional information to that obtained by XRMA and conventional electron microscopic imaging can be obtained by means of electron energy loss spectroscopy. However, elements in small concentrations (i.e. below typically 1 % atomic weight) are difficult to analyze and map in sections thicker than 50-60 nm, using 100 kV primary voltage. Surprisingly, analysis of calcium can be successfully performed on thicker sections though the edge lies above the carbon K edge while it is not possible for the phosphorus edge which is located at lower energies. This is likely due to the edge shapes (sharp for calcium and delayed for phosphorus), and to the more intense contribution of multiple low loss scattering in the background for phosphorus between 100 and 130 eV.

Anhydrous techniques of tissue preparation in combination with imaging possibilities of EELS will provide a new type of information which might lead us to better understanding the etiology and function of structures such as mdg.

## Acknowledgments

We would like to express our sincere thanks to Marianne Engström and Ingeborg May for skilful technical assistance. This work was supported by the Swedish Medical Research Council (proj. no. 00718 and 03355), the King Gustav V 80th Birthday Fund, the King Gustav V Jubilee Fund, the Wenner-Gren Center Funds and the Karolinska Institutet Funds.

## References

Barnard T. (1981). Mitochondrial matrix granules, dense particles and the sequestration of calcium in mitochondria. Scanning Electron Microsc. 1981; II, 419-433.

Barnard T, Ruusa J. (1979). Mitochondrial matrix granules in soft tissues. I Elemental composition by X-ray microanalysis. Exp. Cell Res. 124, 339-347.

Blaineau S, Nicaise G. (1976). Strontium accumulation in atrial muscle cells. J. Microsc. Biol. Cell. 26, 127-132.

Blaineau S, Juliard AK, Amsellem J, Nicaise G. (1987). Quantitative X-ray microanalysis of calcium with the Camebax-TEM system in frozen, freeze-substituted and resin-embedded tissue sections. Application to molluscan glio-interstitial granules. Histochem. 87, 545-555.

Bonnet N, Colliex C, Mory C and Tencé M. (1988) Developments in processing image sequences for elemental mapping. Scanning Microscopy Supplement 2, 351-364.

Egerton RF. (1986). Electron Energy Loss Spectroscopy in the Electron Microscope. Plenum Press, New York.

Hertsens RC, Bernaert I, Joniau M, Jacob WA. (1986). Immunocytochemical investigation of native matrix granules of the rat heart mitochondrion. J. Ultrastruct. Mol. Struct . Res. 94, 1-15.

Jeanguillaume C, Colliex C, Trebbia P. (1978). About the use of electron energy loss spectroscopy for chemical mapping of thin foils with high spatial resolution? Ultramicroscopy 3, 137-142.

Marshall AT. (1980) Freeze-substitution as a preparation technique for biological X-ray microanalysis. Scanning Electr. Microsc. 1980; II, 395-408.

Nicaise G, Gillot I, Julliard AK, Keicher E, Blaineau S, Amsellem J, Meyran JC, Hernandez-Nicaise, Ciapa B, Gleyzal C. (1989) X-ray microanalysis of calcium containing organelles in resin embedded tissue. Scanning Microsc. 3, 199-220

Peachey LD. (1964). Electron microscopic observations on the accumulation of divalent cation in intramitochondrial granules. J. Cell Biol. 20, 95-109.

Sampson HW, Dill RE, Matthews JL, Martin JH. (1970). An electron microscopic localization of calcium-dependent granules in the rat neutrophils. Brain Res. 22, 157-162.

Sevéus L, Brdiczka D, Barnard T. (1978). On the occurrence and the composition of dense particles in mitochondria in ultrathin frozen dry sections. Cell Biol. Int. Rep. 2, 155-162.

Somlyo AP. (1985). Cell calcium measurements with electron probe and electron energy loss analysis. Cell Calcium 6, 197-212.

Somlyo AV, Shuman H, Somlyo AP. (1977). Elemental distribution in striated muscle and the effects of hypertonicity: electron probe analysis of cryo sections. J. Cell. Biol. 74, 828-857.

Stufin LV, Holtorp ME, Ogilvie RE. (1971). Microanalysis of individual mitochondrial granules with diameters less than 1000 Ångströms. Science 174, 947-949.

Trebbia P. (1988). Unbiased methods for signal estimation in electron energy loss spectroscopy, concentration measurements and detection limits in quantitative microanalysis: methods and programs. Ultramicroscopy 24, 399-408.

Trebbia P, Mory C. (1990). EELS elemental mapping with unconventional methods. Part II: Application to biological specimens. Ultramicroscopy 34, 179-203.

Trump BF, Berezesky I. (1986) Evaluation of electron microscopic changes in pathologic material. Electr. Microscopy III, Biology I (eds. Imura T, Maruse S, Suzuki T), 2109-2112.

Wróblewski R. (1989). *In situ* elemental analysis and visualization in cryofixed nervous tissues: X-ray microanalytical investigations of embryological and mature brain, inner ear, photoreceptors, muscle and muscle spindle. Comparison of preparation methods for analysis and visualization at cellular and subcellular levels. J. Microsc. (Oxford) 155, 81-112.

Wróblewski R, Anniko M, Edström L. (1981). A new type of striated muscle in mammalian body: morphological, histochemical, and X-ray microanalytical observations of stapedial muscle in guinea pig. J. Ultrastruct. Res. 76, 46-56.

Wróblewski R, Anniko M, Sakai T. (1984). An unique striated muscle. Further morphological and X-ray microanalytical investigation of the stapedius muscle of the guinea pig using thin and thick cryosections. J. Submicrosc. Cyt. 16, 479-485.

Wróblewski R, Wroblewski J. (1984). Freeze drying and freeze substitution combined with low temperature-embedding: Preparation techniques for microprobe analysis of biological soft tissues. Histochemistry 81, 469-475.

## Discussion with Reviewers

G Nicaise: Glycerol is indeed hydrophilic so we used to shake it in a vial with recently dehydrated molecular sieve just before pouring it in the trough, which contained itself pellets of molecular sieve (Nicaise et al. 1989), Could you specify how you dealt with this problem ? We found (Meyran et al. 1986, Tissue &Cell 18, 276) that ethylene glycol was easier to use.
Authors: We did it almost in the same way as you described. Besides we have been cutting sections on glycerol mainly during the period of late Autumn - early Spring, when the central heating system is on. That significantly decreases problems with humidity in the air during the cutting of plastic sections on glycerol and also of thin cryosections.

G Nicaise: After collecting the sections, one has to get rid of glycerol which would otherwise uncontrollably increase the background (we did it with absolute ethanol which is itself hydrophilic): how did you cope with that?
Authors: Glycerol was removed from the sections with filter paper or pure ethanol. Using ethanol rinse gives nice sections with a low background. However, as you mention yourself rinsing with ethanol which is hydrophilic might introduce further artefacts. We usually try to remove as much as possible of glycerol mechanically and rest of it by drying.

G Nicaise: Could you precise how quantitative the measurements of Fig. 2 are, (id. for the number related to the elemental loss during different cutting procedures).
Authors: The numbers given are ratios between relative peak intensities (peak to background) of phosphorus (P) and calcium (Ca). 5-10 measurements were done in each type of section. The P/Ca ratio in mdg in dry cut sections was 1:1 and in sections cut onto glycerol 1:0.2. In sections cut on water and immediately picked up, the losses of calcium, chlorine and potassium from the mdg were almost complete. Obtained results indicate that strictly anhydrous techniques have to be employed in preparation of biological material for elemental analysis.

Reviewer I: Other EELS workers have given much better limits of detectability for the elements mentioned in this paper (Ca and P). While I do not question the authors´ conclusions, I would appreciate some discussion on this point.
Authors: The spectra shown in Fig. 5 and used for control tests of the EELS quantitation method have been recorded under specific experimental conditions: specimen thickness = 50 nm, beam current = 1 nA, sequential acquisition system with 0.38 s per channel over 1024 channels and energy increments of 0.49 eV/channel. The quoted detection limits correspond to those which could be expected for this specific specimen and these experimental conditions; more specifically the algorithm developed by Trebbia takes into account the quality of the fit (parameter h) for the background modelization. It is therefore not surprising that these detectability limits for the Ca and P are worse than those which can be predicted, in the $10^{-5}$ range, under ideal conditions (PEELS, more intense primary beams).

W.C de Bruijn: In the instructions of other LTVEP-type of instruments much longer drying cycles are recommended: is there any information about the tissue elemental- or structural preservation and the dwell times at certain temperatures ?
Authors: Freeze-drying procedure depends on several factors e.g., temperature of specimen, temperature of condenser, distance between specimen and condenser and the vacuum applied. We found that procedure used by us (Wroblewski 1989) gives superior elemental and structural preservation.

W.C de Bruijn: At the time of introduction around 1964, of the "with water miscible embedding media" like the types now used for low-temperature embedding procedures, we were very much surprised that at the ambient temperature these liquids were even better lipid solvents than the ones that had to be replaced (e.g. acetone). Is there any information about the removal of tissue lipids during infiltration at reduced temperatures? In the paper there is a remark on the lack of visibility of mitochondrial membranes.
Authors: Weibull et al. in a serie of publications (1983, 1984 and 1986) described lipid losses during conventional preparation procedures for electron microscopy and during freeze-substitution. To our knowledge there is no study of that type performed on freeze-dried and vacuum embedded material. The Lowicryl used in present study was of type HM23 which is a hydrophobic type (not water miscible). Poor visibility of the mitochondrial membranes might be due to the very thin section and the fact that no contrasting with heavy metals has been applied. Anhydrous preparation with dry cutting procedure might be the cause of poor visualisation as cutting on a dry knife might "smear" membranes. The membranes do, however, appear "intact" after standard contrasting with uranyl and lead solutions.

W.C de Bruijn: The (improved) stability of the dry sections when observed in the VG-HB 501 as compared to the JEOL 1200 CX is mentioned. One did not mention the stability of the mdg in the beam. From calcium oxalate monohydrate crystals it is known that their stability in the beam is rather poor. Can the authors comment on this point, especially in relation to the results shown in Fig. 6 (356 eV).
Authors: Mdg are stable under the beam in both analytical systems used. The ratio between phosphorus and calcium was constant as well.

W.C de Bruijn: In Fig. 6, I would prefer to have some elemental indication, say P, C and Ca to be added to the rows (2-4). Please provide information about spot size, dwell time per point, number of points per image and energy width of slit. Please explain why you included two pictures taken at 338 eV.
Authors: This is a sequence of 12 micrographs (one annular dark field and 11 energy filtered images) acquired for the simultaneous mapping of phosphorus ($L_{23}$ edge at 135 eV), carbon K edge at 284 eV) and calcium ($L_{23}$ edge at 350 eV). The first two rows contain the data necessary for the P map: the edge is of the delayed type with a maximum at about 160 eV. Consequently the background is estimated from the three first ones at 123, 128 and 135 eV, the signal from the sum of the two images at 150 and 163 eV images. The third row presents the data for the extraction of the carbon signal (pre-edge images at 253 and 279 eV and carbon K image at 338 eV - spectrum in Fig. 3 shows that there is still a large carbon signal of carbon at this energy loss). Moreover, as shown in row 4, the 338 eV can also be chosen at the pre-edge image for the Ca map. In this latter case, as most of the Ca signal is contained in a narrow energy window containing $L_{23}$ line (see Fig. 3), the background contribution is evaluated linearly between the pre-edge image (338 eV) and the post-edge image (356 eV). The results of the extraction of the characteristic Ca and C signals are shown in Fig. 4. All micrographs are 128 x 128 digital images with 4 nm pixel to pixel distance. The probe intensity is about 1 nA within a 3 nm diameter. The energy slit width is 6 eV. Dwell time per pixel and energy loss is 2.9 ms for the phosphorus sequence (average number of $10^4$ counts per pixel) and 9.8 ms for the carbon and calcium sequences (average number of 3500 counts per pixel). The total recording

time for the sequence of image is slightly above 17 min. The corresponding dose is about 2.5 x 107 $e^-/nm^2$. Neither change, nor drift of the specimen have been observed over the total period of acquisition, at the involved resolution level (i.e. 5-10 nm).

## Additional References

Weibull C, Christiansson A, Carlemalm E. (1983). Extraction of membrane lipids during fixation, dehydration and embedding of *Acholeplasma laidlawi*-cells for electron microscopy. J. Microsc. 129, 201-207.

Weibull C, Villiger W, Carlemalm E. (1984). Extraction of lipids during freeze-substitution of *Acholeplasma laidlawi*-cells for electron microscopy. J. Microsc. 134, 213-216.

Weibull C, Christiansson A (1986). Extraction of membrane lipids during low temperature embedding of biological material for electron microscopy. J. Microsc. 142, 79-86.